

UCSF

UC San Francisco Previously Published Works

Title

Evaluation of a New Catheter for Simultaneous Intracranial Pressure Monitoring and Cerebral Spinal Fluid Drainage: A Pilot Study

Permalink

<https://escholarship.org/uc/item/91v4v032>

Authors

Liu, Xiuyun
Zimmermann, Lara L
Ho, Nhi
et al.

Publication Date

2018-12-05

DOI

10.1007/s12028-018-0648-z

Data Availability


The data associated with this publication are available upon request.

Peer reviewed

ORIGINAL ARTICLE



Evaluation of a New Catheter for Simultaneous Intracranial Pressure Monitoring and Cerebral Spinal Fluid Drainage: A Pilot Study

Xiuyun Liu^{1*} , Lara L. Zimmermann², Nhi Ho¹, Paul Vespa³, Xiaoling Liao⁴ and Xiao Hu^{1,3,5,6}

© 2018 Springer Science+Business Media, LLC, part of Springer Nature and Neurocritical Care Society

Abstract

Objectives: Intracranial pressure (ICP) monitoring is a common practice when treating intracranial pathology with risk of elevated ICP. External ventricular drain (EVD) insertion is a standard approach for both monitoring ICP and draining cerebrospinal fluid (CSF). However, the conventional EVD cannot serve these two purposes simultaneously because it cannot accurately measure ICP and its pulsatile waveform while the EVD is open to CSF drainage. A new Integra[®] Camino[®] FLEX Ventricular Catheter (Integra Lifesciences, County Offaly, Ireland) with a double-lumen construction has been recently introduced into the market, and it can monitor ICP waveforms even during CSF drainage. The aim of this study was to evaluate and validate this new FLEX catheter for ICP monitoring in a neurological intensive care unit.

Methods: Six patients with 34 EVD open/close episodes were retrospectively analyzed. Continuous ICP was detected in two ways: through the FLEX sensor at the tip (ICP_f) and through a fluid-coupled manometer within the FLEX catheter, functioning as a conventional EVD (ICP_e). The morphologies of ICP_f and ICP_e pulses were extracted using Morphological Clustering and Analysis of ICP algorithm, an algorithm that has been validated in previous publications. The mean ICP and waveform shapes of ICP pulses detected through the two systems were compared. Bland–Altman plots were used to assess the agreement of the two systems.

Results: A significant linear relationship existed between mean ICP_f and mean ICP_e, which can be described as: $mICP_f = 0.81 \times mICP_e + 1.67$ ($r = 0.79$). The Bland–Altman plot revealed that no significant difference existed between the two ICPs (average of [ICP_e–ICP_f] was -1.69 mmHg, 95% limits of agreement: -7.94 to 4.56 mmHg). The amplitudes of the landmarks of ICP pulse waveforms from the two systems showed strong, linear relationship (r ranging from 0.89 to 0.94).

Conclusions: This study compared a new FLEX ventricular catheter with conventional fluid-coupled manometer for ICP waveform monitoring. Strong concordance in ICP value and waveform morphology between the two systems indicates that this catheter can be used for reliability for both clinical and research applications.

Keywords: External ventricular drainage, Intracranial pressure waveform, Cerebrospinal fluid

*Correspondence: xiuyun.liu@ucsf.edu

¹ Department of Physiological Nursing, University of California, 2 Koret Way, San Francisco, CA 94143, USA

Full list of author information is available at the end of the article

Introduction

Intracranial pressure (ICP) is a complex variable, which is used to derive information about cerebral perfusion pressure, cerebral compensatory mechanisms, cerebral autoregulation, and cerebral arterial changes [1–5]. Elevated ICP is associated with mortality and poor clinical outcome in traumatic brain injury patients (TBI), subarachnoid hemorrhage patients (SAH), and others [6–9]. Therefore, the ability to continuously monitor ICP, analyze ICP waveform, and derive cerebral indices is pivotal in understanding pathology, targeting therapy, and predicting prognosis [10–12]. The technique most commonly used in clinical practice to monitor ICP involves external ventricular drain (EVD) and intraparenchymal pressure monitor, while the latter only allows ICP monitoring without a combined therapeutic option of cerebrospinal fluid (CSF) drainage [13]. EVD has become a gold standard in a neurological intensive care unit (NICU) for both monitoring ICP and diverting CSF from the ventricles to reduce ICP [14–16]. EVD insertion is proved to be valuable, indeed often lifesaving, in intraventricular hemorrhage (IVH), SAH, TBI, and bacterial meningitis [14, 17, 18]. However, the conventional EVD system, with one side inserted to ventricle and the other side connected to a collection reservoir to allow for drainage of CSF or to a pressure transducer [19], is not able to simultaneously record ICP pulse waveforms while it is open to drain CSF [14, 20]. As a consequence, either a second ICP sensor needs to be used or intermittent closure of EVD is applied to spot check ICP [20]. Both approaches are not desirable. The first approach introduces additional risk of having a second invasive probe, and the second approach introduces additional burden on health care providers and may miss important information due to intermittent nature of the measurement [21].

Recently, a novel ventricular catheter, branded as Integra® Camino® FLEX Ventricular Catheter (Integra Lifesciences, County Offaly, Ireland), has been introduced into the market [22]. This double-lumen catheter uses one lumen to divert CSF and the other to embed a pressure sensor at the tip of the catheter to obtain ICP pulse waveforms (Fig. 1a), thus enabling continuous ICP monitoring even when EVD is open. The aim of this study was to validate the new FLEX catheter by comparing ICP recordings obtained through this new catheter with recordings obtained using conventional EVD. The interpretation of ICP using a single number, for example mean value, although useful, can sometimes be misleading. A high-resolution view of ICP waveforms is needed for more sophisticated analysis of ICP [1]. Therefore, both the mean values and the waveform shapes (P_1 , P_2 , and P_3 , as shown in Fig. 2) of the ICP recordings were studied in this article.

Methods

Patients and Data Collection

The data analyzed in this study were collected from adult patients admitted to University of California, Los Angeles Medical Center (UCLA, Los Angeles, CA, USA), during a period of evaluating Integra® Camino® FLEX Ventricular Catheter (Integra Lifesciences, County Offaly, Ireland) between February and April 2016. Three patients with severe TBI (a loss of consciousness of greater than 6 h and a Glasgow Coma Scale of 3–8), two patients with aneurysmal subarachnoid hemorrhage (aSAH), and one patient with IVH were enrolled in the study. ICP was continuously monitored in two ways: through the FLEX sensor at the tip (ICP_t) and through a fluid-coupled manometer connected with FLEX catheter, functioning as a conventional EVD (ICP_e). In order to make the article concise, the term ‘EVD’ was used instead of the ‘fluid-coupled manometer’ in the remaining part of this article. The electrocardiograph data were recorded by GE Solaris 8000 (Little Chalfont, United Kingdom) patient monitor. All the signals were obtained using BedMaster™ (Excel Medical, Jupiter, Florida, USA) system at a sampling rate of 240 Hz. The institutional review board approved the data analysis and waived the need for consenting patients because of the retrospective nature of the study. The decision to use FLEX catheters was clinically based without considering the needs of this study.

We retrospectively reviewed ICP recordings from each patient and selected the episodes associated with acute CSF drainage that caused ICP reduction (34 episodes in total from the six subjects). For each episode, we identified timing of EVD opening (t_0) and closure (t_1) based on the timing points when ICP_e became a flat line after EVD is open. A during-drainage segment was defined as the segment while EVD is open to CSF drainage, i.e., from t_0 to t_1 (Fig. 1b). A pre-drainage segment was defined as the segment of ICP prior to EVD opening. A post-drainage segment is defined as the segment after EVD is closed again (Fig. 1b).

Data Analysis

In this study, we investigated the differences between ICP_t and ICP_e in both the mean values and the morphological features of the ICP pulse waveforms. A modern computational algorithm, the Morphological Clustering and Analysis of ICP (MOCAIP) algorithm, was used to extract the morphological features of an ICP pulse, including pulse amplitude, time intervals among sub-peaks, curvature, slope, and decay time constants (shown in Fig. 2). The algorithm has been validated in our previous publications [5, 23–25].

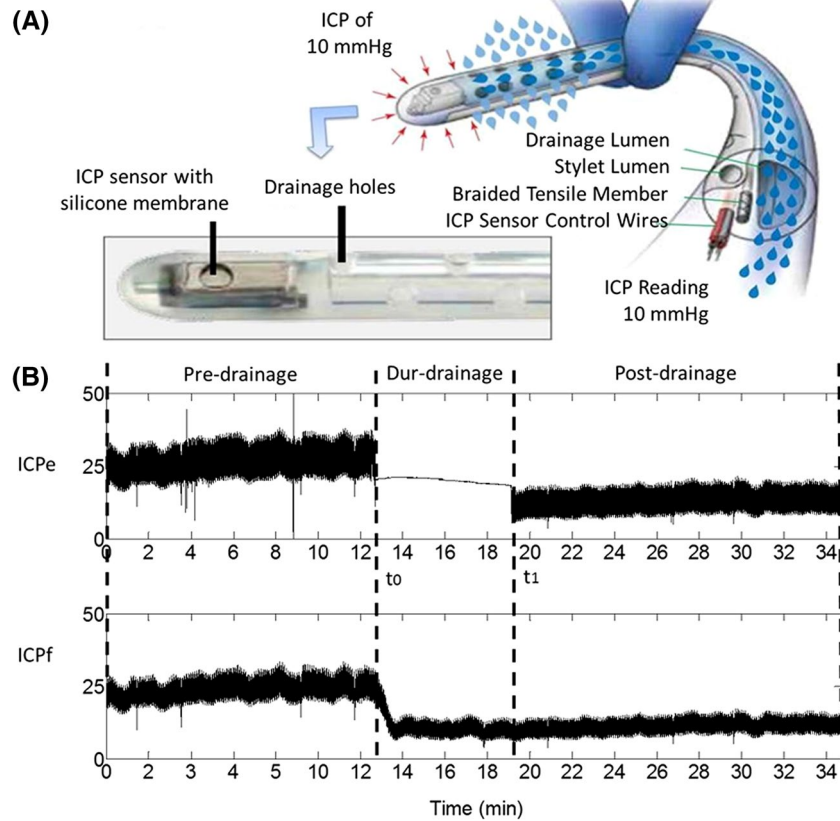


Fig. 1 **a** Structure of FLEX double-lumen catheter. Sensor located at the tip of the catheter allows continuous ICP measurement in the ventricle. This graph has been adapted from the original figure with the permission of the manufacture [22]. **b** Segments of the ICP recordings from the built-in sensor of the FLEX ventricular catheter at the top (ICP_i) and from the external manometer coupled with the drainage lumen of the FLEX catheter (ICP_e). The during-drainage segment refers to segment between [t_0 , t_1], the pre-drainage segment was a segment of ICP prior to EVD opening, and the post-drainage segment refers to the segment after closing EVD again. *EVD* external ventricular drain, *ICP* intracranial pressure

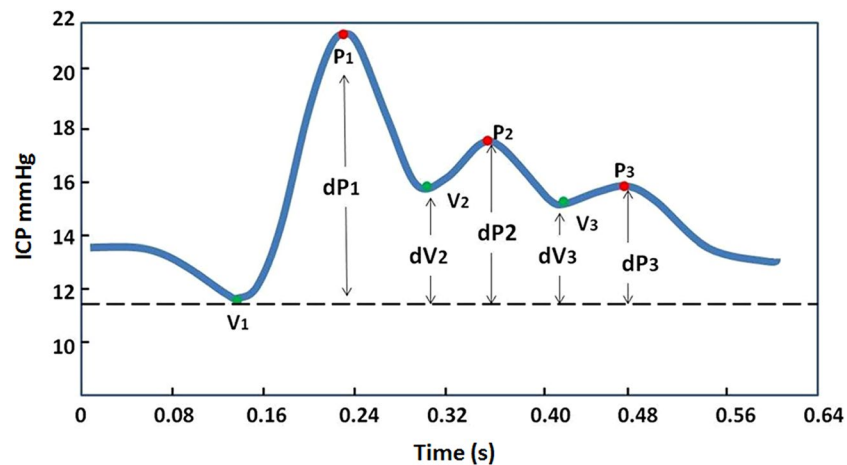


Fig. 2 MOCAIP algorithm can systematically calculate 128 metrics that are related to the amplitude, time interval, curvature, slope, and decay time constants based on the landmarks identified on an ICP pulse. P₁, P₂, and P₃: three peaks of ICP; V₁, V₂, and V₃: three valleys of ICP waves. *MOCAIP* morphological clustering and analysis of intracranial pulse, *ICP* intracranial pressure

Briefly, the process for using the MOCAIP includes, (1) analyzing a segment of ICP signal to produce a sequence of consecutive raw ICP pulses [25]; (2) clustering the raw ICP pulses into distinct groups based on their morphological distance, in order to exclude uncertain noise and artifacts; (3) identifying the largest cluster and calculating the averaged pulse of this largest cluster, termed dominant ICP pulse [26]; (4) recognizing legitimate dominant pulses, using a reference library of validated ICP pulses, as described in our original publication [24]; (5) the MOCAIP algorithm performs a comprehensive search for all landmark points on an ICP pulse and uses them as candidates for designating the three subpeaks; and (6) finally, the best designation of the three well-recognized ICP subpeaks (P_1 , P_2 , and P_3) is obtained for each validated pulse [5]. As Table 1 summarizes, 128 pulse morphological metrics are extracted using the identified peaks and troughs of the pulse. A schematic intracranial pulse is shown in Fig. 2. Hu et al. discuss further details of the MOCAIP algorithm [24].

Waveforms of ICP_f and ICP_e during pre- and post-drainage section of each EVD-opening/closure episode were analyzed. One dominant wave was produced every 12 s. The mean ICP and the amplitudes of P_1 , P_2 , and P_3 and V_1 , V_2 , and V_3 were compared.

Statistical Analysis

Statistical analysis was performed using the IBM SPSS Statistics (version 21) software. Spearman's correlation coefficient (r) was used to study the cross-relationship between mean value of dominant waves of ICP_e and ICP_f ($n=4273$). Correlation coefficient r was also calculated

between the amplitudes of the six landmarks of pulses of ICP_e and ICP_f . Bland–Altman plots were used to investigate the agreement of the mean ICP of the two sensing systems.

Results

Patient Demographics and Summary Statistics

The mean age of the six (three males) patients enrolled in the study was 41.2 ± 19.1 (mean \pm SD) years. Thirty-four ICP episodes with EVD opening/closure were selected. The number of episodes selected from each subject varies from 1 to 11 ($N_1=5$, $N_2=10$, $N_3=2$, $N_4=5$, $N_5=11$, $N_6=1$), and this variation reflects the clinical decisions made at the time of patient monitoring with regard to the needs of opening EVD. The mean recording time of selected EVD opening/closure episode was 47.8 ± 9.4 min (mean \pm SD), ranging from 25.3 to 60.2 min. Mean ICP and mean amplitude of six landmarks of ICP pulses detected by the two sensing systems in pre- and post-CSF drainage periods are shown in Table 2.

Mean ICP Detected via FLEX Catheter and Conventional EVD

We first compared the mean value of each ICP dominant wave detected by the two approaches (ICP_e and ICP_f). There was a linear relationship between the two ICPs, which can be approximated by a linear equation: $mICP_f = 0.81 \times mICP_e + 1.67$ ($r=0.79$, Fig. 3a). The Bland–Altman plot (Fig. 3b) reveals no significant difference between the two ICPs, with mean ($ICP_e - ICP_f$) being -1.69 mmHg and the limits of agreement being -7.94 – 4.56 mmHg.

Table 1 Description of the 128 metrics derived from the six landmarks detected by MOCAIP algorithm on a pulse of CBFV

Metric group index	Notation	Description
1	$dV_1, dV_2, dV_3, dP_1, dP_2, dP_3$	Amplitude of the landmarks relative to the minimum point prior to initial rise
2	$L_{V1P1}, L_{V1P2}, L_{V1P3}, L_{V2P2}, L_{V3P3}$	Time delay among landmarks
3	$Curv_{V1}, Curv_{V2}, Curv_{V3}, Curv_{P1}, Curv_{P2}, Curv_{P3}$	Absolute curvature of each landmark
4	$K_1, K_2, K_3, RC_1, RC_2, RC_3$	K_1, K_2, K_3 are slopes of each rising edge and RC_1, RC_2, RC_3 are time constants of each descending edge
5	$mCBFV, dias\ CBFV$	Mean CBFV and diastolic CBFV
6	L_T	Time delay of V_1 to ECG QRS peak
7	$mCurv$	Mean absolute curvature of the pulse
8	$WaveAmp$	Maximum among dP_1 and dP_3
9	dP_{P1P2}, \dots	Ratio among landmark amplitudes
10	$L_{V1P1}/L_T, \dots$	Ratio among time delays
11	$Curv_{V1}/Curv_{V2}, \dots$	Ratio among curvatures
12	$K_1/RC_1, \dots$	Ratio among slopes/RCS

The 28 metrics belonging to groups of 1–8 are called basic metrics, while the remaining 100 metrics (belonging to groups of 9–12) are extended metrics calculated as ratios among basic metrics within each group

CBFV cerebral blood flow velocity, ECG electrocardiograph, MOCAIP morphological clustering and analysis of intracranial pulse

Table 2 Mean ICP (unit: mmHg), mean amplitude (dP₁ to dP₃, dV₁ to dV₃, unit: mmHg), and time delay (L_{V1P1}, L_{V1P2}, L_{V1P3}, L_{V2P2}, L_{V3P3}, unit: ms) of six landmarks of ICP waveforms pre- and post-CSF drainage

mICP	dP ₁	dP ₂	dP ₃	dV ₁	dV ₂	dV ₃	L _{V1P1}	L _{V1P2}	L _{V1P3}	L _{V2P2}	L _{V3P3}	
ICP waveform pre- and post-CSF drainage detected by EVD												
Pre-	16.16 ± 2.56	4.41 ± 2.73	4.58 ± 2.31	3.72 ± 1.71	0.017 ± 0.02	3.32 ± 1.62	3.35 ± 1.58	84.81 ± 16.69	212.39 ± 26.56	328.35 ± 35.22	72.33 ± 13.11	56.90 ± 15.14
Post-	12.93 ± 4.73	3.81 ± 2.69	3.71 ± 2.24	2.97 ± 1.78	0.019 ± 0.02	2.73 ± 1.55	2.68 ± 1.63	75.96 ± 26.0	190.94 ± 60.14	306.65 ± 89.33	63.91 ± 25.53	56.66 ± 21.97
ICP waveform pre- and post-CSF drainage detected by FLEX catheter												
Pre-	16.14 ± 2.18	3.33 ± 1.82	4.22 ± 1.92	3.51 ± 1.57	0.011 ± 0.01	3.37 ± 1.72	3.42 ± 1.61	108.19 ± 16.98	222.71 ± 30.39	327.69 ± 42.54	66.40 ± 20.45	48.17 ± 13.56
Post-	13.57 ± 2.05	2.99 ± 1.55	3.43 ± 1.76	2.82 ± 1.43	0.012 ± 0.01	2.87 ± 1.50	2.53 ± 1.78	111.23 ± 27.47	215.10 ± 34.12	343.44 ± 20.99	61.25 ± 22.46	56.57 ± 12.36

P₁, P₂, and P₃: three peaks of ICP; V₁, V₂, and V₃: three valleys of ICP waves. dV₁, dV₂, dV₃, dP₁, dP₂, and dP₃: amplitudes of landmarks relative to the minimum point prior to initial rise. L_{V1P1}, L_{V1P2}, L_{V1P3}, L_{V2P2}, and L_{V3P3}: time delay among landmarks

CSF cerebrospinal fluid, ICP intracranial pressure

Morphological Shapes of the ICP Pulse Waveforms Detected by the Two Systems

We then compared the morphological features of ICP_e and ICP_f. Qualitatively, the waveforms of ICP_f are slightly different from those recorded using EVD (ICP_e) as shown in Fig. 4, where one pair of ICP pulses per patient is randomly selected from the pre-drainage segment, from FLEX catheter (blue), and from EVD (red). To perform a quantitative comparison, we calculated the amplitudes of each dominant ICP pulse at the six landmarks (P₁ through P₃ and V₁ through V₃). Six scatter plots between pairs of these landmarks from the two sensing systems are displayed in Fig. 5. Each color represents one patient in the future. Except the first valley point (V₁), the other five landmarks of ICP pulses showed strong correlation as indicated by large r ranging from 0.89 to 0.94. Interestingly, for dP₁, different cohorts of patients have different gradients (Fig. 5a).

Discussion

Continuous ICP monitoring remains a useful tool in the management of patients in NICU [27, 28]. A significant reason for death and long-term disability due to head injuries and other intracranial pathological conditions is an elevation in the ICP [1]. A continuous and accurate measurement of ICP as part of the neurological armamentarium is important in understanding disturbances in brain function. Although EVD is still considered to be the gold standard for ICP monitoring, it may miss important information of ICP while it is open to CSF drainage [29]. Therefore, in clinical practice, there are times when both intraparenchymal ICP monitor (IPM) and EVD are placed in the same patient [30]. Several studies compared the ICP measurements from IPM and EVD, and their conclusions vary. Some studies suggest ICP data from the two devices are not interchangeable [30, 31], while others show good agreement between ICP readings from IPM and EVD [21, 32]. A system that can serve the needs of ICP monitoring and CSF drainage simultaneously is highly desirable, such as Integra® Camino® FLEX Ventricular Catheter used in this study. To our knowledge, we presented the first-ever study validating the FLEX ventricular catheter. Our results showed a linear relationship between mean ICP recorded through FLEX catheter (ICP_f) and conventional EVD (ICP_e). There is no significant difference between the two systems. According to the standards for ICP monitoring devices developed by American National Standards Institute/Association for the Advancement of Medical Instrumentation (ANSI/AAMI, <http://www.aami.org/>) [33], ICP monitoring devices should provide an accuracy of 2 mmHg in the range of 0–20 mmHg, and the maximum error should

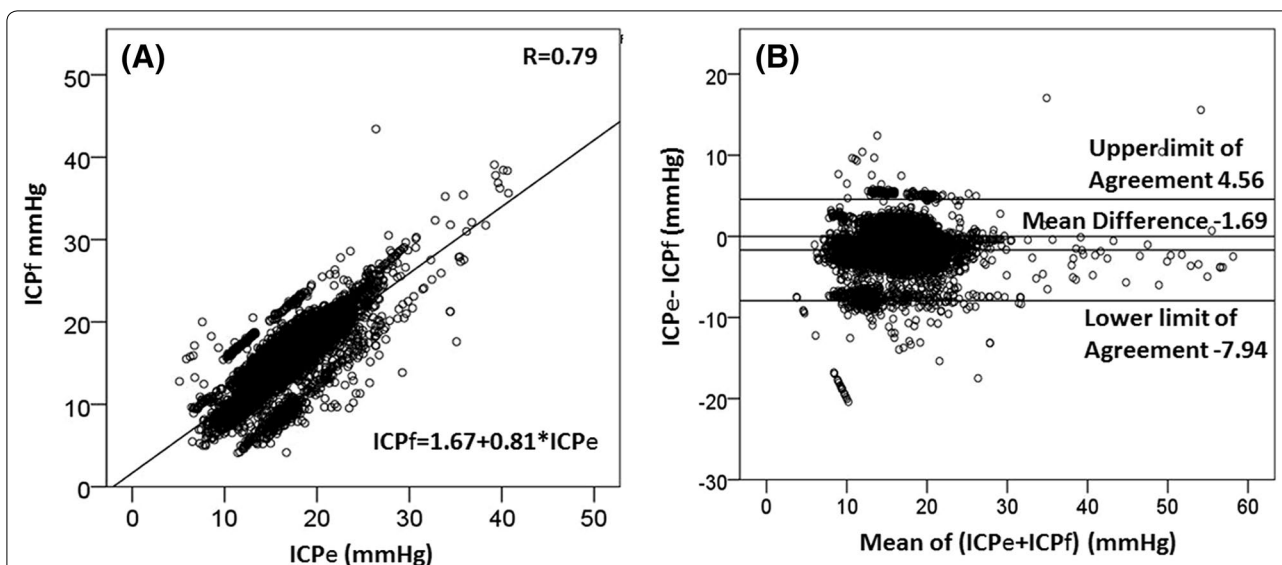


Fig. 3 **a** A scatter plot between mean ICP from the conventional EVD (x -axis, ICP_e) and from FLEX sensor at the tip (y -axis, ICP_f) ($n=4273$). A significant linear correlation was found between the two ICPs. **b** Bland-Altman plot between the two ICP measurements indicates that mean difference between the two ICPs is only -1.96 mmHg. 95% confidence interval of agreement is -7.94 to 4.56 mmHg. *ICP* intracranial pressure, *EVD* external ventricular drains

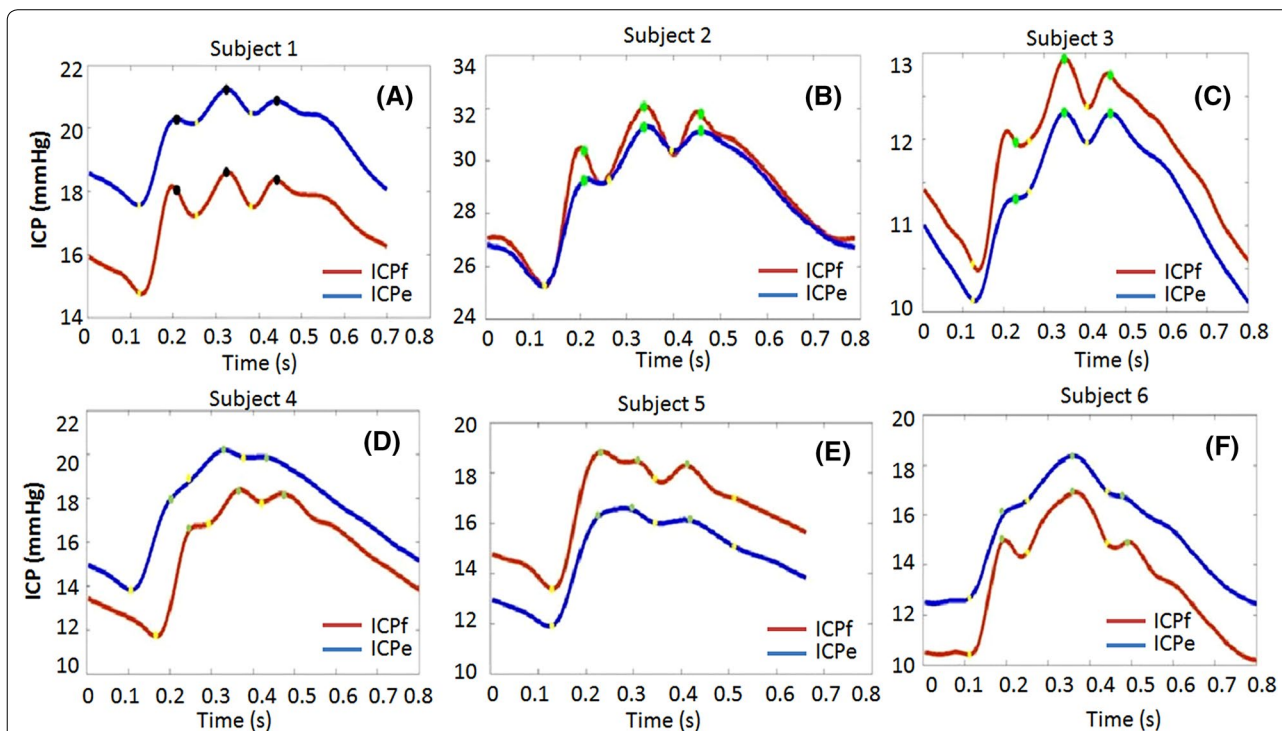
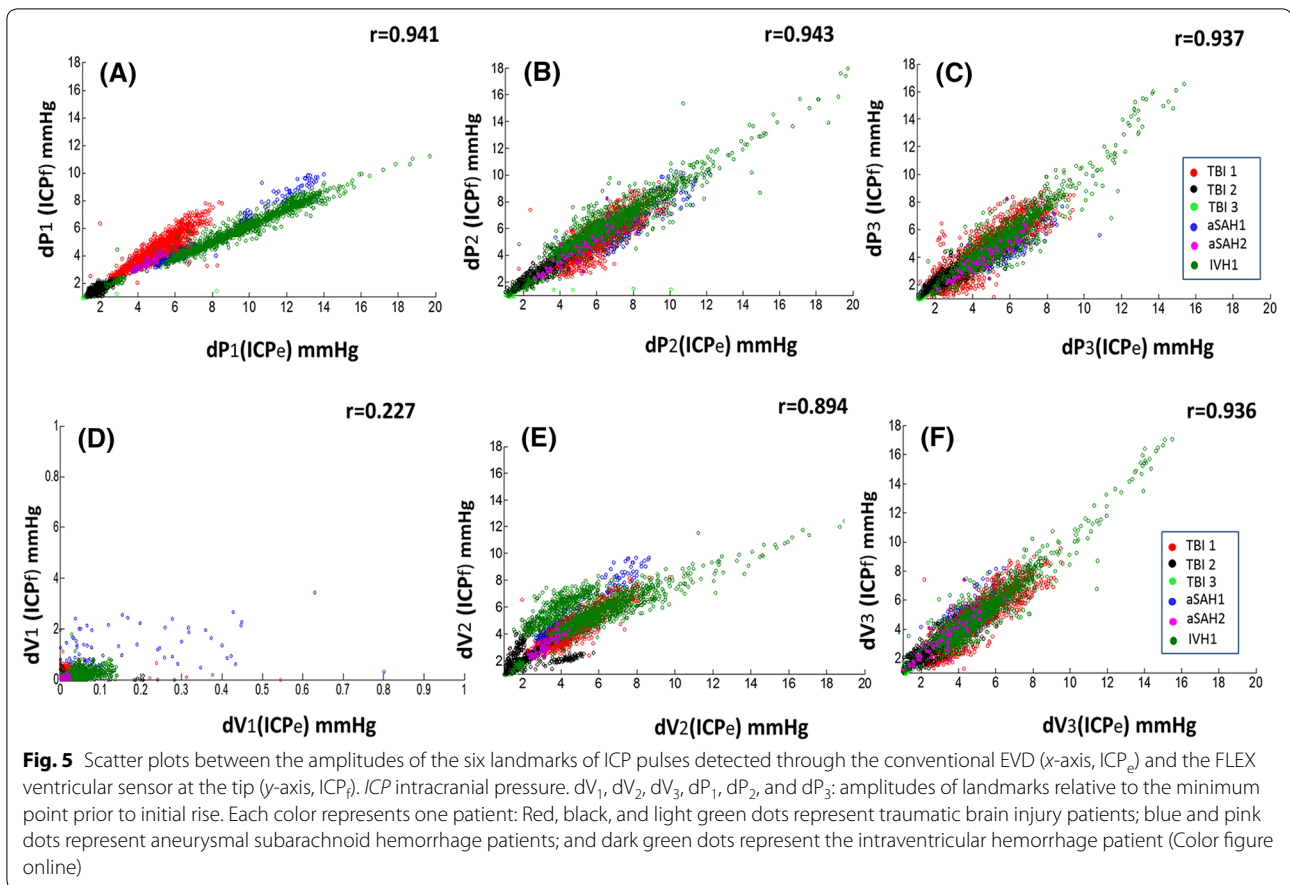


Fig. 4 Comparison of ICP pulse waveforms recorded by FLEX ventricular sensor (red) and by the conventional EVD sensor (blue). Each figure represents one dominant ICP pulse randomly selected from each subject. *ICP*: intracranial pressure; *EVD*: external ventricular drains (Color figure online)



not exceed 10% in the range of 20–100 mmHg. The mean difference of 1.69 mmHg between ICP_e and ICP_f in our study is within the 2 mmHg tolerance level required by the ANSI/AAMI standard and can be considered as a surrogate of conventional EVD for ICP monitoring.

Besides mean value, ICP waveform morphology should be considered when assessing reliability of ICP monitors [21, 34]. The ICP pulse waveforms, characterized by three notches (P_1 , P_2 , P_3), also contain pathological information. The percussion wave (P_1) represents arterial pulsation; the tidal wave (P_2) represents intracranial compliance; and the dicrotic wave (P_3) represents aortic valve closure [35–37]. Increased amplitudes of all three peak waves are related to elevated mean ICP caused by increased CSF, increased amplitude of P_1 might be related to increased systolic ABP, and increased amplitude of P_2 would be due to decreased intracranial compliance. It is important to compare the morphological difference of ICP pulses recorded by the FLEX catheter and EVD in this study. The MOCAIP algorithm was used to extract the morphological features of ICP waveforms. This algorithm has been validated in several studies including a study related to normal subjects' response

under hypercapnia challenge [23], a study of cerebral vascular changes among TBI patients related to lactate pyruvate ratio increase [38], and a study of cerebral vascular changes in response to electroencephalogram (EEG) bursts among severe brain injury patients under an EEG burst suppression states [39]. These existing studies have shown the validity of the MOCAIP algorithm and prove its feasibility to be used in our present research.

By comparing the metrics derived through the MOCAIP algorithm, we found that the six landmarks of ICP pulses from the two sensing systems were highly correlated. The weakest correlation was found in the first valley point (V_1) of ICP_e and ICP_f . However, the value of V_1 was extremely tiny compared with the amplitudes of other features, and the absolute difference between V_1 amplitude of ICP_e and ICP_f was small enough to be negligible (0.012 mmHg). Interestingly, for dP_1 , different cohorts of patients have different gradients as shown in Fig. 5a; the TBI cohort (red, black, and light green dots) displays bigger gradient than aSAH patients (pink and blue dots) and the ICH patient (dark green dots). Although morphological features of ICP_e and ICP_f were highly correlated, the ICP pulses from the two systems

were distinctively different. Therefore, it is important to avoid directly mixing shapes of ICP pulses from EVD and the FLEX ventricular catheter. It looks like the contours of ICP_f are more well defined than ICP_e (Fig. 4), and this difference might be due to different digital or analog filter settings on bedside patient monitors for acquiring these two signals, or might be because of the different measurement systems: The FLEX catheter detects ICP through sensor at the tip located in the ventricle while EVD detected the ICP using fluid-coupled device that may have dampened the ICP pulse. On the other hand, Fig. 4 might suggest that FLEX catheter is more sensitive to ICP changes and it is superior to conventional fluid-coupled ICP sensing.

This study validated the usage of FLEX catheter for ICP monitoring, which can provide more information about ICP even during CSF drainage and can avoid missing events of elevated ICP. For conventional EVD, nurses need to intermittently clamp the EVD to measure ICP. This operation not only increases the clinician burden, but also needs professional training to the nurses. Standard guideline requires at least 30-s to 1-min wait before reading ICP values during intermittent ICP checking [14], due to the reason that ICP dynamics have inherent hysteresis and require a certain amount of time to reach a new equilibrium after closing the system to CSF drainage. Inaccurate assessment of ICP can impact treatment decisions and impact patient outcomes. The FLEX catheter releases this clinical burden through continuous monitoring of ICP. Moreover, as the sensor of FLEX system is located at the tip inserted into the ventricle, it can still monitor ICP even when CSF drainage cannot be established due to slit or shifted ventricles or becomes occluded due to bloody CSF. As the FLEX catheter monitors ICP directly at the source, it provides an accurate reading regardless of patient position. The nurses do not need to frequently realign the transducer every time while they change the patient's position [22]. With more information of ICP obtained during CSF drainage, it is possible to analyze vascular changes and flow dynamics by using advanced algorithms, such as MOCAIP, which still needs further study in the future.

Finally, we acknowledge the following limitations. Firstly, the patient population in the present study was rather small (only six patients). Future study with more data is needed. Moreover, as our main aim of this project was to study the cerebral vascular changes in response to acute ICP decrease, we only analyzed the episodes with acute decrease in ICP during CSF drainage, a short period before CSF drainage (baseline), and a short period after CSF drainage. However, not the whole long recordings of ICP signals during patient's

stay in hospital were analyzed. Therefore, if the catheter tip ICP sensor had long-term drifting in its accuracy, in theory, it would lead to larger difference between the mean ICP from this sensor and the mean ICP acquired by using conventional EVD. Therefore, our selection of EVD-opening episodes might not be able to detect this phenomenon as frequent EVD opening to drain CSF may occur more often in the acute phase of ICP monitoring. However, there are uncertainties in terms of the maintenance of an accurate calibration of fluid-coupled device throughout the monitoring. Therefore, we would argue that future prospective studies that take into consideration of all these factors are needed to investigate whether catheter tip sensors have long-term drifting. Thirdly, the price of FLEX catheter is higher than the conventional EVD; however, with more information about ICP, this FLEX system avoids intermittent ICP checking and reduces the clinical burden. It also allows us to further study the cerebral dynamics in different situations, especially during CSF drainage with acute ICP drop.

Conclusions

This study compared a new FLEX ventricular catheter with conventional fluid-coupled manometer for ICP waveform monitoring. Strong concordance in ICP value and waveform morphology between the two systems indicates that this catheter can be used for reliability for both clinical and research applications.

Author details

¹ Department of Physiological Nursing, University of California, 2 Koret Way, San Francisco, CA 94143, USA. ² Department of Neurology Surgery, University of California, Davis, USA. ³ Department of Neurosurgery, School of Medicine, University of California, Los Angeles, USA. ⁴ Chongqing Engineering Laboratory of Nano/Micro Biological Medicine Detection Technology, Institute of Biomedical Engineering, Chongqing University of Science and Technology, Chongqing, People's Republic of China. ⁵ Department of Neurological Surgery, University of California, San Francisco, USA. ⁶ Institute of Computational Health Sciences, University of California, San Francisco, USA.

Author Contributions

The concept and study design were formed by XH, XYL, PV, LZ, and XLL. Data acquisition was conducted by PV, NH, and LZ. Data analysis was conducted by XYL, NH, XLL, and XH. Drafting of the manuscript and figures was contributed by XYL, XH, LZ, PV, NH, and XLL.

Source of support

This work was partially supported by the UCSF Middle Career Scientist Award, UCSF Institute for Computational Health Sciences, and National Institutes of Health Awards R01NS076738 and NS106905-01A1.

Compliance with Ethical Standards

Conflict of interest

The authors declare that they have no conflict of interest.

Ethical approval and Informed consent

The institutional review board (IRB) approved the data analysis and waived the need for consenting patients because of the retrospective nature of the study.

Published online: 03 December 2018

References

1. Kawoos U, McCarron RM, Auker CR, Chavko M. Advances in intracranial pressure monitoring and its significance in managing traumatic brain injury. *Int J Mol Sci.* 2015;16:28979–97.
2. Donnelly J, Budohoski KP, Smielewski P, Czosnyka M. Regulation of the cerebral circulation: bedside assessment and clinical implications. *Crit Care.* 2016;20:129.
3. Hu X, Glenn T, Scalzo F, Bergsneider M, Sarkiss C, Martin N, et al. Intracranial pressure pulse morphological features improved detection of decreased cerebral blood flow. *Physiol Meas.* 2010;31:679–95.
4. Kim MO, Adji A, O'Rourke MF, Avolio AP, Smielewski P, Pickard JD, et al. Principles of cerebral hemodynamics when intracranial pressure is raised: lessons from the peripheral circulation. *J Hypertens.* 2015;33:1233–41.
5. Asgari S, Gonzalez N, Subudhi AW, Hamilton R, Vespa P, Bergsneider M, et al. Continuous detection of cerebral vasodilatation and vasoconstriction using intracranial pulse morphological template matching. *PLoS One.* 2012;7:e50795.
6. Czosnyka M, Pickard J. Monitoring and interpretation of intracranial pressure. *J Neurol Neurosurg Psychiatry.* 2004;75:813–21.
7. Wainwright MS, Lewandowski R. Bioinformatics analysis of mortality associated with elevated intracranial pressure in children. *Intracranial Press Brain Monit.* 2012;14:67–73.
8. Zoerle T, Lombardo A, Colombo A, Longhi L, Zanier ER, Rampini P, et al. Intracranial pressure after subarachnoid hemorrhage. *Crit Care Med.* 2014;43:168–76.
9. Shen L, Wang Z, Su Z, Qiu S, Xu J, Zhou Y, et al. Effects of intracranial pressure monitoring on mortality in patients with severe traumatic brain injury: a meta-analysis. *PLoS One.* 2016;11:e0168901.
10. Rangel-Castillo L, Robertson CS. Management of intracranial hypertension. *Crit Care Clin.* 2006;22(4):713–32.
11. Liu X, Maurits N, Aries M, Czosnyka M, Ercole A, Donnelly J, et al. Monitoring of optimal cerebral perfusion pressure in traumatic brain injured patients using a multi-window weighting algorithm. *J Neurotrauma.* 2017;34:3081–8.
12. Chari A, Dasgupta D, Smedley A, Craven C, Dyson E, Matloob S, et al. Intraparenchymal intracranial pressure monitoring for hydrocephalus and cerebrospinal fluid disorders. *Acta Neurochir (Wien).* 2017;159:1967–78.
13. Robinson JD. Management of refractory intracranial pressure. *Crit Care Nurs Clin North Am.* 2016;28:67–75.
14. Muralidharan R. External ventricular drains: management and complications. *Surg Neurol Int.* 2015;6:271.
15. Kirmani A, Sarmast A, Bhat A. Role of external ventricular drainage in the management of intraventricular hemorrhage; its complications and management. *Surg Neurol Int.* 2015;6:188.
16. Staykov D, Kuramatsu JB, Bardutzky J, Volbers B, Gerner ST, Kloska SP, et al. Efficacy and safety of combined intraventricular fibrinolysis with lumbar drainage for prevention of permanent shunt dependency after intracerebral hemorrhage with severe ventricular involvement: a randomized trial and individual patient data meta-analysis. *Ann Neurol.* 2017;81:93–103.
17. Griesdale DEG, McEwen J, Kurth T, Chittock DR. External ventricular drains and mortality in patients with severe traumatic brain injury. *Can J Neurol Sci.* 2010;37:43–8.
18. Lovasik BP, McCracken DJ, McCracken CE, McDougal ME, Frerich JM, Samuels OB, et al. The effect of external ventricular drain use in intracerebral hemorrhage. *World Neurosurg.* 2016;94:309–18.
19. de Andrade AF, Paiva WS, Neville IS, Noleto GS, Alves Junior A, Sandon LHD, et al. Monoblock external ventricular drainage system in the treatment of patients with acute hydrocephalus: a pilot study. *Med Sci Monit.* 2014;20:227.
20. Slazinski T, Anderson TA, Cattell E, Eigsti JE, Heimsoth S, Holleman J. Care of the patient undergoing intracranial pressure monitoring/external ventricular drainage or lumbar drainage. *Am Assoc Neurosci Nurs.* 2011;43:1–38.
21. Berlin T, Murray-Krezaan C, Yonas H. Comparison of parenchymal and ventricular intracranial pressure readings utilizing a novel multi-parameter intracranial access system. *Springerplus.* 2015;4:1–8.
22. Integra Lifesciences. Integra design verification report for camino flex ventricular catheter. 2013. Retrieved from <https://www.integralife.com/file/general/1453796957.pdf>.
23. Asgari S, Bergsneider M, Hamilton R, Vespa P, Hu X. Consistent changes in intracranial pressure waveform morphology induced by acute hypercapnic cerebral vasodilatation. *Neurocrit Care.* 2011;15:55–62.
24. Hu X, Xu P, Scalzo F, Vespa P, Bergsneider M. Morphological clustering and analysis of continuous intracranial pressure. *IEEE Trans Biomed Eng.* 2009;56:696–705.
25. Hu X, Xu P, Lee DJ, Vespa P, Baldwin K, Bergsneider M. An algorithm for extracting intracranial pressure latency relative to electrocardiogram R wave. *Physiol Meas.* 2008;29:459–71.
26. Hu X, Xu P, Asgari S, Vespa P, Bergsneider M. Forecasting ICP elevation based on prescient changes of intracranial pressure waveform morphology. *IEEE Trans Biomed Eng.* 2010;57:1070–8.
27. Trauner DA, Brown F, Ganz E, Huttenlocher PR. Treatment of elevated intracranial pressure in reye syndrome. *Ann Neurol.* 1978;4:275–8.
28. Hawthorne C, Piper I. Monitoring of intracranial pressure in patients with traumatic brain injury. *Front Neurol.* 2014;5:121.
29. Zhong J, Dujovny M, Park HK, Perez E, Perlin AR, Diaz FG. Advances in ICP monitoring techniques. *Neurol Res.* 2003;25:339–50.
30. Mahdavi ZK, Olson DM, Figueroa SA. Association patterns of simultaneous intraventricular and intraparenchymal intracranial pressure measurements. *Neurosurgery.* 2016;79:561–6.
31. Brean A, Eide PK, Stubhaug A. Comparison of intracranial pressure measured simultaneously within the brain parenchyma and cerebral ventricles. *J Clin Monit Comput.* 2006;20:411–4.
32. Chambers IR, Siddique MS, Banister K, Mendelow AD. Clinical comparison of the Spiegelberg parenchymal transducer and ventricular fluid pressure. *J Neurol Neurosurg Psychiatry.* 2001;71:383–5.
33. American National Standards Institute. Intracranial pressure monitoring devices. American National Standards Institute: Arlington; 1993. p. 1993.
34. Littlejohns L, Bader M. AACN-AACN protocols for practice: monitoring technologies in critically ill neuroscience patients. Sudbury: Jones and Bartlett; 2008.
35. Kirkness CJ, Mitchell PH, Burr RL, March KS, Newell DW. Intracranial pressure waveform analysis: clinical and research implications. *J Neurosci Nurs.* 2000;32:271–7.
36. Smith M. Monitoring intracranial pressure in traumatic brain injury. *Anesth Analg.* 2008;106:240–8.
37. Raboel PH, Bartek J, Andresen M, Bellander BM, Romner B. Intracranial pressure monitoring: invasive versus non-invasive methods—a review. *Crit Care Res Pract.* 2012. <https://doi.org/10.1155/2012/950393>.
38. Asgari S, Vespa P, Bergsneider M, Hu X. Lack of consistent intracranial pressure pulse morphological changes during episodes of microdialysis lactate/pyruvate ratio increase. *Physiol Meas.* 2011;32:1639–51.
39. Connolly M, Vespa P, Hu X. Characterization of cerebral vascular response to EEG bursts using ICP pulse waveform template matching. *Acta Neurochir Suppl.* 2016;122:291–4.